Bioactive Constituents, Metabolites, and Functions

3,4-Seco-Dammarane Triterpenoid Saponins with Anti-inflammatory Activity Isolated from the Leaves of Cyclocarya paliurus

Wei Liu, Shengping Deng, Dexiong Zhou, Yan Huang, Chenguo Li, Lili Hao, Gaorong Zhang, Shanshan Su, Xia Xu, Rui-Yun Yang, Jun Li, and Xishan Huang

J. Agric. Food Chem., **Just Accepted Manuscript** • DOI: 10.1021/acs.jafc.9b06898 • Publication Date (Web): 22 Jan 2020

3,4-*Seco*-Dammarane Triterpenoid Saponins with Anti-inflammatory Activity Isolated from the Leaves of *Cyclocarya paliurus*

Wei Liu, Shengping Deng, Dexiong Zhou, Yan Huang, Chenguo Li, Lili Hao, Gaorong Zhang, Shanshan Su, Xia Xu, Ruiyun Yang, Jun Li *, Xishan Huang*

State Key Laboratory for the Chemistry and Molecular Engineering of Medicinal Resources, School of Chemistry and Pharmaceutical Sciences of Guangxi Normal University, Guilin 541004, China

ABSTRACT: *Cyclocarya paliurus*is commonly used for the prevention and treatment of hypertension, diabetes, and inflammation in South China. Although research on the anti-inflammatory effects of *C. paliurus* leaves has been reported, no active anti-inflammatory compounds have been identified. In the present study, RAW 264.7 cells were used to establish a bioactivity-guided identification model to verify the inhibitory effects of *C. paliurus* leaves on inflammation and identify the anti-inflammatory constituents. The active fraction was isolated to yield eighteen dammarane triterpenoid saponins, including eleven new 3,4-*seco*-dammarane triterpenoid saponins (**1-11**), the structures of which were identified on the basis of analyses of nuclear magnetic resonance (NMR) spectroscopy, mass spectrometry (MS) and comparison with literature data. Compounds **7**, **8**, **10**, and **11** showed strong inhibition on nitric oxide (NO) productions, with IC_{50} values ranging from 8.23 μM to 11.23 μM. These four compounds significantly decreased the secretion of tumor necrosis factor-alpha (TNF-α), prostaglandin E_2 (PGE_2) and interleukin 6 (IL-6) in lipopolysaccharide (LPS)-activated RAW 264.7 cells. Furthermore, compound **7** decreased the expression of the proteins cyclooxygenase-2 (COX-2), inducible nitric-oxide synthase (iNOS), and nuclear factor kappa-B (NF-κB/p65). In addition,

the structure-activity relationships of the isolates were investigated. The results suggest that 3,4-*seco*-dammarane triterpenoid saponins may be used as potential anti-inflammatory drugs and warrant further investigation.

INTRODUCTION

Cyclocarya paliurus (Batal.) Iljinskaja, a Chinese indigenous plant, is the sole species in the genus *Cyclocarya* Iljinskaja of the Juglandaceae family. The leaves of *C. paliurus* are used not only as drug formulations in traditional Chinese medicine to treat hyperlipidemia, hypertension, diabetes mellitus, chronic inflammatory diseases and as an antioxidant but also as a famous "sweet tea", with a very sweet taste, in folk medicine in China to prevent and treat hypertension, diabetes, and inflammation.[1-6] The leaves of *C. paliurus* were approved as a new raw food material by The National Health Commission of the People's Republic of China in 2013.[7] Currently, *C. paliurus* is an important and valuable crop in the functional food market. A variety of triterpenoid glycosides, flavonoids, and other compounds have been isolated from the leaves of this plant.[8] Among its constituents, 3,4-*seco*-dammarane triterpenoids are considered characteristic taxonomic indicators of this plant and the primary active and functional constituents in *C. paliurus*. To date, 20 *seco*-dammarane triterpenoid glycosides, which are cleaved in plants by hydroxylation or methyl esterification at C-3 and C-4 followed by glycosylation at C-12, have been reported.[9-14] Some of them have a sweet taste and are used as functional food ingredients. For example, cyclocariosides I-II are approximately 50 to 100 times sweeter than 2% sucrose[15-16] and are used as sweeteners and antitumor agents.[17] Although research on the anti-inflammatory effects of an extract of *C. paliurus* has been reported,[18] no active anti-inflammatory compound has been reported. To explore potential bioactive

compounds from the leaves of *C. paliurus*, a bioactivity-guided investigation of anti-inflammatory compounds was carried out. The active fraction was isolated to yield eleven new 3,4-*seco*-dammarane triterpenoid saponins (**1**−**11**) and seven known dammarane triterpenoid saponins (**12**−**18**) (Figure 1). The inhibition of NO by the extracts and compounds were evaluated. Furthermore, the effects of the anti-inflammatory compounds on the levels of inflammatory cytokines TNF-α, PGE_2 and IL-6 and the expression of proteins iNOS, COX-2 and NF-κB/p65 were tested using LPS-activated RAW 264.7 macrophage cells. We describe herein the separation and structural identification of *seco*-dammarane triterpenoid saponins, their anti-inflammatory effects, and their structure-activity relationships.

MATERIALS AND METHODS

Instruments. The detailed experimental instruments are seen in the Support Information (Text S1).

Chemicals. Silica gel (Qingdao Marine Chemical Co., Ltd., China), Sephadex LH-20 gel (Amersham Pharmacia Biotech AB, Sweden), and RP-C_{18} (Merck, Germany) were used for various separations. D-glucose, L-glucose, L-arabinose, D-arabinose, D-quinovose, and L-quinovose were used as the sugar standards (Sigma-Aldrich, Munich, Germany).

Plant materials. The leaves (20.0 kg) of *C. paliurus* were bought from Xiushui county, Jiangxi Province, China in July 2017 and identified by Associate Professor Qiang Xie (Guangxi Normal University). A specimen (No. ID-20170705) was preserved in the State Key Laboratory of Medicinal Resources of Guangxi Normal University.

Preparation of extracts and isolation of triterpenoid saponins. The fresh, dried

leaves (20.0 kg) of *C. paliurus* were extracted with 75% ethanol (EtOH, 4 × 3 h), and the solvent was evaporated under vacuum to obtain an extract. The crude extract (2.0 kg) was suspended in distilled water and partitioned with polyethylene (PE), ethyl acetate (EtOAc) and n-butanol (*n*-BuOH) to obtain a PE extract (480 g), an EtOAc extract (450 g) and an *n*-BuOH extract (600 g). The anti-inflammatory effects were analyzed by measuring the inhibition of NO production in LPS-activated RAW 264.7 cells.

The active EtOAc fraction was loaded to a chromatography column (CC) on silica gel eluted with CH_2Cl_2-MeOH mixtures (from 1:0 to 0:1) to yield eight fractions (Fr. A to Fr. H). The anti-inflammatory fraction D (45 g) was fractionated using an MCI gel CC eluting with MeOH-H_2O (from 3:7 to 1:0) to obtain Fr. D-1 to Fr. D-4. Fr. D-3 (10 g) was further separated using RP-C_{18} CC eluting with gradients of MeOH-H_2O (from 6:10 to 1:0) to afford Fr. D-3-1 to Fr. D-3-4. Fr. D-3-2 (0.8 g) was loaded to Sephadex LH-20 eluting with gradients of H_2O-MeOH (from 1:0 to 0:1), and further separated by RP-C_{18} semi-preparative HPLC to furnish compounds **1** (28.0 mg), **2** (15.4 mg), and **3** (7.1 mg). Fr. D-3-3 (3.2 g) was applied to Sephadex LH-20 CC and eluted with MeOH and then chromatographed with semi-preparative RP-C_{18} HPLC to afford compounds **4** (28.0 mg), **5** (15.2 mg), and **13** (30.3 mg). Fr. D-3-4 (4.2 g) was chromatographed by silica gel and eluted with gradients of CH_2Cl_2-MeOH (from 1:0 to 0:1) to create Fr. D-3-4-1 to Fr. D-3-4-5. Fr. D-3-4-2 was subjected to Sephadex LH-20 CC and RP-C_{18} HPLC to get compounds **6** (28.2 mg), **7** (15.2 mg), **11** (11.4 mg), and **12** (1.0 mg). In addition, Fr. D-3-4-3 was isolated by Sephadex LH-20 CC and RP-C_{18} HPLC to afford compounds **8** (28.2 mg), **9** (15.0 mg), and **10** (19.7 mg). The anti-inflammatory Fr. E (80 g) was subjected to MCI gel eluting with gradients of MeOH-H_2O (from 6:4 to 1:0) to yield Fr. E-1 to Fr. E-4. Active Fr. E-3 (23 g) was

101 further chromatographed by RP-C_{18} CC eluted with gradients of MeOH-H_2O (from
102 6:10 to 1:0) to afford Fr. E-3-1 to Fr. E-3-4. Fr. E-3-2 was subjected to Sephadex
103 LH-20 CC and semi-preparative RP-C_{18} HPLC to afford compounds **14** (28.3 mg), **15**
104 (15.4 mg), **16** (12.1 mg), **17** (12.0 mg), and **18** (12.3 mg).

105 *Cyclocarioside R (**1**)*: The various chromatographic isolation and purification gave
106 28.0 mg of white, amorphous powder; $[\alpha]_D^{25}$ + 38.0 (*c* 0.16, MeOH); negative
107 HRESIMS *m/z* calculated for $C_{36}H_{60}ClO_{10}$ [M + Cl] $^-$, 687.3859, found: 687.3875;
108 ^{1}H- (500 MHz) and ^{13}C-NMR (125 MHz) data (pyridine-d_5, Tables 1 and 3).

109 *Cyclocarioside S (**2**)*: The various chromatographic isolation and purification gave
110 15.4 mg of white, amorphous powder; $[\alpha]_D^{25}$ + 28.6 (*c* 0.12, MeOH); positive
111 HRESIMS *m/z* calculated for $C_{36}H_{60}O_{10}Na$ [M + Na] $^+$, 675.4073, found: 675.4084;
112 ^{1}H- (500 MHz) and ^{13}C-NMR (125 MHz) data (pyridine-d_5, Tables 1 and 3).

113 *Cyclocarioside T (**3**)*: The various chromatographic isolation and purification gave
114 7.1 mg of white, amorphous powder; $[\alpha]_D^{25}$ + 10.6 (*c* 0.19, MeOH); negative
115 HRESIMS *m/z* calculated for $C_{37}H_{62}ClO_{10}$ [M + Cl] $^-$, 701.4142, found: 701.4032;
116 ^{1}H- (500 MHz) and ^{13}C-NMR (125 MHz) data (pyridine-d_5, Tables 1 and 3).

117 *Cyclocarioside U (**4**)*: The various chromatographic isolation and purification gave
118 28.0 mg of white, amorphous powder; $[\alpha]_D^{25}$ + 27.6 (*c* 0.14, MeOH); positive
119 HRESIMS *m/z* calculated for $C_{36}H_{45}O_4$ [M + Na] $^+$, 641.4069, found: 641.4029; ^{1}H-
120 (500 MHz) and ^{13}C-NMR (125 MHz) data (pyridine-d_5, Tables 1 and 3).

121 *Cyclocarioside V (**5**)*: The various chromatographic isolation and purification gave
122 15.2 mg of white, amorphous powder; $[\alpha]_D^{25}$ + 4.8 (*c* 0.14, MeOH); negative
123 HRESIMS *m/z* calculated for $C_{37}H_{60}ClO_8$ [M + Cl] $^-$, 667.3960, found: 667.3977; ^{1}H-
124 (500 MHz) and ^{13}C-NMR (125 MHz) data (pyridine-d_5, Tables 1 and 3).

125 *Cyclocarioside W (**6**)*: The various chromatographic isolation and purification gave

28.2 mg of white, amorphous powder; $[\alpha]_D^{25}$ + 11.3 (c 0.14, MeOH); positive HRESIMS *m/z* calculated for $C_{37}H_{60}O_9Na$ [M + Na] $^+$, 671.4136, found: 671.4135; ^{1}H- (500 MHz) and ^{13}C-NMR (125 MHz) data (pyridine-d_5, Tables 1 and 3).

*Cyclocarioside X (**7**)*: The various chromatographic isolation and purification gave 15.2 mg of white, amorphous powder; $[\alpha]_D^{25}$ + 24.8 (*c* 0.07, MeOH); negative HRESIMS *m/z* calculated for $C_{37}H_{62}ClO_9$ [M + Cl] $^-$, 685.4074, found: 685.4082; ^{1}H- (500 MHz) and ^{13}C-NMR (125 MHz) data (pyridine-d_5, Tables 2 and 3).

*Cyclocarioside Y (**8**)*: The various chromatographic isolation and purification gave 28.2 mg of white, amorphous powder; $[\alpha]_D^{25}$ + 1.5 (*c* 0.14, MeOH); positive HRESIMS *m/z* calculated for $C_{38}H_{64}O_9Na$ [M + Na] $^+$, 687.4491, found: 687.4448; ^{1}H- (500 MHz) and ^{13}C-NMR (125 MHz) data (pyridine-d_5, Tables 2 and 3).

*Cyclocarioside Z_1 (**9**)*: The various chromatographic isolation and purification gave 15.0 mg of white, amorphous powder; $[\alpha]_D^{25}$ + 2.9 (*c* 0.19, MeOH); positive HRESIMS *m/z* calculated for $C_{37}H_{62}O_9Na$ [M + Na] $^+$, 673.4279, found: 673.4292; ^{1}H- (500 MHz) and ^{13}C-NMR (125 MHz) data (pyridine-d_5, Tables 2 and 3).

*Cyclocarioside Z_2 (**10**)*: The various chromatographic isolation and purification gave 19.7 mg of white, amorphous powder; $[\alpha]_D^{25}$ + 34.0 (*c* 0.10, MeOH); negative HRESIMS *m/z* calculated for $C_{37}H_{62}ClO_9$ [M + Cl] $^-$, 685.4072, found: 685.4082; ^{1}H- (500 MHz) and ^{13}C-NMR (125 MHz) data (pyridine-d_5, Tables 2 and 3).

*Cyclocarioside Z_3 (**11**)*: The various chromatographic isolation and purification gave 11.4 mg of white, amorphous powder; $[\alpha]_D^{25}$ + 38.9 (*c* 0.14, MeOH); negative HRESIMS *m/z* calculated for $C_{38}H_{64}ClO_9$ [M + Cl] $^-$, 699.422, found: 699.4239; ^{1}H- (500 MHz) and ^{13}C-NMR (125 MHz) data (pyridine-d_5, Tables 2 and 3).

Determination of the absolute configurations of the sugars. Each new compound was dissolved in 1 M HCl and stirred at 80 °C for 2 hours. The solution of

the reactant was then extracted with EtOAc 3 times. The H_2O layers were evaporated under vacuum. The presence of L-arabinose in the aqueous layers of compounds **1**, **2**, **4**, **7**, and **10** were detected by Sigel TLC (H_2O-MeOH-CH_2Cl_2, 1:8:12) with standard sample. D-quinovose was confirmed as the sugar moiety of compounds **3**, **5**, **8**, **9** and **11** by Sigel TLC (H_2O-MeOH-CH_2Cl_2, 1:8:12) with standard sample, and D-glucose was identified as the sugar moiety of compound **6** by Sigel TLC (H_2O-MeOH-CH_2Cl_2, 1:8:12) with standard sample.

Cell viability. RAW 264.7 cell viability was performed using the previously described MTT method.[19] The detailed procedures are seen in the Support Information (Text S2).

NO production assay. NO production was detected according to a previous report.[20] The detailed procedures are seen in the Support Information (Text S3).

Enzyme-linked immunosorbent assay (ELISA). The expression of proinflammatory cytokines (TNF-α, PGE_2, and IL-6) was tested using the previously described method.[21] The detailed procedures are seen in the Support Information (Text S4).

Western blotting analysis. The expressions of proteins iNOS, NF-κB/p65, and COX-2 were assayed by Western blotting analysis according to standard procedures published previously.[19] The detailed procedures are seen in the Support Information (Text S5).

Statistical analysis. All data were performed by Student's test. The results are displayed as the mean ± standard deviation (SD) for three independent experiments. Differences were considered statistically significant at $p < 0.05$.

RESULTS AND DISCUSSION

Structural elucidation of the 3,4-*seco*-dammarane triterpenoid saponins.

Cyclocarioside R (**1**) yielded a negative-ion peak $[M + Cl]^-$ at *m/z* 687.3859 (calcd. for $C_{36}H_{60}ClO_{10}$, 687.3875) in its HRESIMS spectrum (Figure S1), which demonstrated a molecular formula, $C_{36}H_{60}O_{10}$, in light of its 1D NMR (pyridine-d_5) and HRESIMS data. The ^{1}H NMR data (pyridine-d_5, Table 1) of **1** exhibited six methyl signals at δ_H 0.96 (s, 30-CH_3), 1.02 (s, 18-CH_3), 1.24 (s, 19-CH_3), 1.58 (s, 21-CH_3), 2.06 (s, 27-CH_3), and 1.80 (s, 29-CH_3); a methoxy group at δ_H 3.51 (s, 3-OMe); two terminal methylene olefinic protons at δ_H 5.33 (br s, H-26a), 5.15 (br s, H-26b), 4.87 (br s, H-28a), and 4.95 (br s, H-28b); and a glycosyl anomeric proton at δ_H 4.80 (d, $J_{H\text{-}1'/H\text{-}2'}$ = 7.4 Hz, H-1'). The ^{13}C-NMR (pyridine-d_5, Table 3) and the distortionless enhancement by polarization transfer (DEPT) (Figure S4) spectra displayed the existence of a carboxyl group (–C=O) at δ_C 176.3 and two terminal double bonds (–C=CH_2) at δ_C 148.9 (C-4), 114.3 (C-28) and δ_C 147.8 (C-25), 113.5 (C-26). The ^{1}H-^{1}H correlation spectroscopy (COSY) (Figures 2 and S6) of **1** demonstrated the presence of four fragments (H-1/H-2, H-5/H-6/H-7, H-11/H-12/ H-13/H-17/H-16/H-15, H-22/H-23/H-24). In its HMBC spectrum (Figures 2 and S7), a key correlation from H-3-OMe (δ_H 3.51, s) to C-3 (δ_C 176.3) suggested that the –OCH_3 connected to C-3. The cross peaks from H-28 (δ_H 4.95, 4.87, br s) to C-5 (δ_C 52.5) and C-29 (δ_C 24.2, s) and from H-26 (δ_H 5.33, 5.15, br s) to C-24 (δ_C 80.9) and C-27 (δ_C 19.1) indicated the two terminal double bonds (–C=CH_2) linked to C-4 and C-25, respectively. The HMBC correlations from H-21-CH_3 (δ_H 1.58, s) to C-17 (δ_C 52.3) confirmed the side chain linked to C-17. The HMBC correlations from the H-1′ (δ_H 4.80, d, anomeric proton) to C-12 (δ_C 75.7) suggested that the arabinopyranose was linked to C-12. Its diagnostic ROESY correlations of H-5/H-9/H-12/H-17/ H-CH_3-21/ H-23/H-CH_3-30 suggested that H-5, H-9, H-12, H-17, CH_3-21, H-23, and

CH_3-30 are α-oriented (Figures 3 and S8). The β-orientations of H-13, H-CH_3-18, and H-CH_3-19 were then verified by the ROESY correlations of H-13/H-CH_3-18 /H-CH_3-19. In addition, the pentose unit was assigned as α-L-arabinopyranosyl based on its ^{1}H-and ^{13}C-NMR data (pyridine-d_5, Tables 1 and 3) and comparison with other 3,4-*seco*-dammarane triterpenoid saponin from this plant[11-13] as well as further hydrolysis of **1** with 1M HCl and Sigel TLC with standard L-arabinose. The coupling constant of $J_{H\text{-}1'/H\text{-}2'}$ = 7.4 Hz of the anomeric proton suggested that the L-arabinose was also α-oriented. Analyses of the 1D and 2D-NMR data of **1** showed high similarity to those of cyclocarioside K,[14] suggesting that **1** includes the basic 3,4-*seco*-dammarane triterpenoid skeleton, differing from cyclocarioside K only in the signals of the side chain. The 20-, 23- and 24-OH substituents were confirmed by the ^{1}H-^{1}H COSY correlations of H-22/H-23/H-24 along with the key HMBC correlations from H-21-CH_3 to C-20 (δ_C 76.2) and C-22 (δ_C 41.9) and from H-23 to C-20 (δ_C 76.2), C-24 (δ_C 80.9) and C-25 (δ_C 147.8) (Figure 2). The above information indicated that **1** was a characteristic 3,4-*seco*-dammarane saponin.

The molecular formula of cyclocarioside S (**2**) was deduced to be $C_{36}H_{60}O_{10}$ based on its sodium adduct molecular ion peak $[M + Na]^+$ at *m/z* 675.4073 (calcd. for $C_{36}H_{60}O_{10}Na$, 675.4084) in its HRESIMS (Figure S9) spectrum, which has the same formula as that of **1**. Compound **2** had almost identical NMR (Tables 1 and 3) data to that of **1**, as revealed by comparisons of their MS and NMR signals. Small differences existed in the ^{1}H- and ^{13}C-NMR (pyridine-d_5) data of positions 22, 23, and 24 between **2** and **1**. The ^{1}H NMR signals of H-22, 23, and 24 shifted from δ_H 1.90, 2.17, 4.54, and 4.40 in **1** to δ_H 2.12, 2.29, 4.61, and 4.57 in **2**, respectively (Table 1). Moreover, the ^{13}C NMR signals of C-22, 23, and 24 shifted from δ_C 41.9, 71.8, and 80.9 in **1** to δ_C 40.1, 71.6, and 79.9 in **2**, respectively (Table 3). Furthermore,

compounds **1** and **2** exhibited two peaks with different retention times in the HPLC chromatogram (Figure S17), indicating that **1** and **2** are epimers. The results indicate that **2** is also a 3,4-*seco*-dammarane triterpenoid saponin.

To assess the relative configurations of positions 23 and 24 in their side chains of **1** and **2**, their ROESY correlations and ^{1}H-^{1}H coupling constant values were focused. The ROESY correlation of H-23/H-CH_3-21 indicated that H-23 and H-CH_3-21 are α-oriented (Figures 3 and S8). Moreover, the ROESY spectrum of **2** (Figures 3 and S16) showed a correlation between H-24/H-CH_3-21, indicating that H-CH_3-21 and H-24 are α-oriented. Furthermore, piscidinol A[22] and 24-*epi*-piscidinol A,[23] which possessed the same eight-carbon side chains as **1** and **2** with *syn* and *anti* orietations between hydrogens at positions 23 and 24, revealed coupling constants of $J \approx 0$ Hz and 8.0 Hz, and their structures were identified by X-ray analysis. Correspondingly, combretanone A,[24] alisol E[25] and 23,24,25-trihydroxycycloartan-3-one,[26] which have *syn* and *anti* orietations between hydrogens at positions 23 and 24, exhibited coupling constants of $J \approx 0$ Hz and 6.0 Hz, respectively. The similar coupling constants of respective $J = 6.4$ Hz and $J = 5.8$ Hz of **1** and **2** between hydrogens at positions 23 and 24 suggested that both hydrogens linked to positions 23 and 24 were in *anti*-configurations. Thus, on the basis of their ROESY correlations and coupling constants between hydrogens at positions 23 and 24, the absolute configurations of carbons at positions 23 and 24 of **1** and **2** were determined as 23*R*, 24*S,* and 23*S*, 24*R,* respectively. Compounds **1** and **2** were named cyclocarioside R and cyclocarioside S*,* respectively (Figure 1).

Cyclocarioside T (**3**) yielded a negative-ion peak $[M + Cl]^-$ at *m/z* 701.4142 (calcd. for $C_{37}H_{62}ClO_{10}$, 701.4132) in its HRESIMS spectrum (Figure S18), which demonstrated a molecular formula, $C_{37}H_{62}O_{10}$, in light of its 1D NMR (pyridine-d_5)

and HRESIMS data. The ^{1}H-, ^{13}C-NMR data (pyridine-d_5, Tables 1 and 3) of **3** were similar to those of compound **1**, indicating that **3** also possesses a similar 3,4-*seco*-dammarane triterpenoid skeleton as **1**, differing only in the presence of a *β*-D-quinovopyranosyl unit at position 12 and the absence of an *α*-L-arabinopyranosyl unit. The sugar unit was identified as a *β*-D-quinovopyranosyl moiety based on the ^{1}H-, ^{13}C-NMR data (pyridine-d_5, Tables 1 and 3), the hydrolysis of **3** with 1M HCl and Sigel TLC with standard sample. In its HMBC spectrum (Figures 2 and S24), the methyl singlets H-6'-CH_3 (δ_H 1.59, d, J = 5.6 Hz) correlated with an oxymethine carbon resonance at C-5' (δ_C 73.3), indicating that H-6'-CH_3 was connected to C-5', and H-1' (δ_H 4.88, d, $J_{H\text{-}1'/H\text{-}2'}$ = 7.9 Hz, a glycosyl anomeric proton) was correlated with C-12 (δ_C 76.3, an oxymethine carbon resonance), suggesting the sugar group was connected to C-12. In the ROESY spectrum of **1**, the correlation of H-CH_3-21/H-23 indicated that H-CH_3-21 and H-23 are *α*-oriented (Figures 3 and S25). Moreover, the coupling constant of J = 6.2 Hz of **3** suggested that H-23 and H-24 were in *anti*-configurations with respect to their configurations in **1**, and the absolute configurations of carbons at positions 23 and 24 of **3** was assigned as 23*R*, 24*S*. Thus, **3** was determined and named cyclocarioside T (Figure 1).

Cyclocarioside U (**4**) yielded a positive-ion peak [M + Na] $^{+}$ at *m/z* 641.4069 (calcd. for $C_{36}H_{58}O_8Na$, 641.4029) in its HRESIMS spectrum (Figure S26), which demonstrated a molecular formula, $C_{36}H_{58}O_8$, in light of its 1D NMR (pyridine-d_5) and HRESIMS data. Its ^{1}H-NMR data (pyridine-d_5, Table 1) exhibited six methyl signals at δ_H 0.95 (s, 30-CH_3), 1.05 (s, 18-CH_3), 1.25 (s, 19-CH_3), 1.49 (s, 21-CH_3), 1.89 (s, 27-CH_3), and 0.95 (s, 29-CH_3); a methoxy signal at δ_H 3.52 (s, 3-OMe); three olefinic protons including two terminal double bond protons at δ_H 6.15 (m, H-23), 6.45 (d, J = 15.7 Hz, H-24); δ_H 5.07 (br s, H-26a), 4.98 (br s, H-26b); and δ_H 4.87 (br

s, H-28a), 4.95 (br s, H-28b); and a glycosyl anomeric proton at δ_H 4.82 (d, $J_{H\text{-}1'/H\text{-}2'}$ = 7.4 Hz, H-1'). Its spectra of ^{13}C-NMR (pyridine-d_5, Table 3) and DEPT (Figure S29) indicated the presence of a carboxyl unit at δ_C 176.3 (C-3) and three double bond signals at δ_C 148.9 (C-4), 114.2 (C-28); δ_C 128.7 (C-23), 135.9 (C-24); and δ_C 143.1 (C-25), 115.4 (C-26). The ^{1}H-, ^{13}C-NMR data (pyridine-d_5) for **4** displayed a number of similarities to those of **1** but differed in the signals of the eight-carbon side chain, indicating that **4** also possesses a 3,4-*seco*-dammarane triterpenoid skeleton. Its ^{1}H-^{1}H COSY (Figures 2 and S31) correlations of H-22 (δ_H 2.58, 2.71, m)/H-23 (δ_H 6.15, m)/H-24 (δ_H 6.45, d, J = 15.7 Hz) suggested the existence of a –CH_2CH=CH– fragment. The HMBC (Figures 2 and S32) correlations of H-23 (δ_H 6.15, m) with C-20 (δ_C 74.9) and H-24 (δ_H 6.45, d, J = 15.7 Hz) with C-26 (δ_C 115.4) and C-27 (δ_C 19.3) indicated the location of the additional double bond is at positions 23 and 24. In addition, the sugar unit was identified as α-L-arabinopyranosyl based on the ^{1}H-, ^{13}C-NMR (pyridine-d_5, Tables 1 and 3) data, the hydrolysis of **4** with 1M HCl and Sigel TLC with L-arabinose, as well as comparison with those of **1**. The L-arabinose is linked to C-12 by the HMBC correlation from H-1′ (anomeric proton) to C-12. Therefore, the structure of **4** was identified and assigned as cyclocarioside U (Figure 1).

The molecular formula of cyclocarioside V (**5**), $C_{37}H_{60}O_8$, was determined by 1D NMR (pyridine-d_5) data and HRESIMS *m/z* 667.3960 $[M + Cl]^-$ (calcd. for $C_{37}H_{60}ClO_8$, 667.3977) (Figure S34), which is 14 Da more than that of **4**. The 1D NMR (pyridine-d_5, Tables 1 and 3) signals of **5** closely resembled those of **4**; they differed in the existence of a –CH_3 at δ_H 1.55 (d, J = 5.6 Hz). Comparisons of the 1D NMR, MS data between **5** and **4** revealed a pronounced difference in the signals for the sugar moiety and the presence of a methyl hexacarbonose in **5**, indicating that **5**

also possesses a 3,4-*seco*-dammarane triterpenoid skeleton. The hydrolysis of **5** with 1M HCl and Sigel TLC with standard sample attributed the sugar in **5** as a quinovopyranose. The arabinopyranose linked to position 12 in **4** was replaced by a quinovopyranose in **5**. The coupling constant of $J_{H\text{-}1'/H\text{-}2'}$ = 7.3 Hz of the anomeric proton, suggested the quinovopyranose was *β*-oriented. In the HMBC spectrum, the correlation of H-6'-CH_3 (δ_H 1.55, d, J = 5.6 Hz) with C-5' (δ_C 73.2) indicated 6'-CH_3 connected to C-5'. The HMBC correlation (Figures 2 and S40) of H-1' (anomeric proton) with C-12 unambiguously confirmed that the sugar unit was situated at C-12. Thus, the structure of **5** was deduced and given the common name cyclocarioside V (Figure 1).

Cyclocarioside W (**6**) yielded a negative-ion peak $[M + Cl]^-$ at *m/z* 671.4136 (calcd. for $C_{37}H_{60}ClO_{10}$, 671.4135) in its HRESIMS spectrum (Figure S42), which demonstrated a molecular formula, $C_{37}H_{60}O_{10}$, in light of its 1D NMR (pyridine-d_5) and HRESIMS data. The 1D NMR (pyridine-d_5, Tables 1 and 3) spectra of **6** were closely similar to those of **5** except for the absence of the –CH_3 peaks [δ_H 1.55 (3H, d, 5.9 Hz); δ_C 18.9] observed in **5** and the existence of alternative –CH_2OH singlets [δ_H 4.38, 4.52 (2H, m); δ_C 63.9] in **6**, suggesting that **6** is also a 3,4-*seco*-dammarane triterpenoid. In the HMBC spectrum (Figures 2 and S48), the correlation of 6'-CH_2OH (δ_H 4.38, 4.52, m) with C-5' (δ_C 72.8) indicated that the –CH_2OH was linked to C-5'. The HMBC correlation of H-1' (δ_H 4.94, anomeric proton) with C-12 (δ_C 76.6) indicated the sugar was connected to C-12. The hydrolysis of **6** with HCl yielded D-glucose as identified by Sigel TLC analysis. The coupling constant of $J_{H\text{-}1'/H\text{-}2'}$ = 7.3 Hz of the glucosyl anomeric proton indicated the *β*-orientation for **6**. Consequently, the structure of **6** was deduced and given the common name cyclocarioside W (Figure 1).

Cyclocarioside X (**7**) yielded a positive-ion peak $[M + Na]^+$ at *m/z* 673.427 in its HRESIMS spectrum (Figure S50), which demonstrated a molecular formula, $C_{37}H_{62}O_9$, in light of its 1D NMR (pyridine-d_5) and HRESIMS data. The 1D NMR spectra (pyridine-d_5, Tables 2 and 3) of **7** were closely analogous to those of **4** except in the signals of their side chains, indicating that **7** also possesses a 3,4-*seco*-dammarane triterpenoid skeleton. There were signals from a methyl group (δ_H 1.34, s; δ_C 26.4, 26-CH_3), a quaternary carbon (δ_C 74.6, C-25) and an additional methoxy group (δ_H 3.24, s; δ_C 50.7, 25-OCH_3) in **7**, replacing the terminal olefin at δ_H 4.95 and 5.01, and at δ_C 115.4 and 143.1 observed in **4**. The HMBC (Figures 2 and S56) correlations from δ_H 3.24 (25-OCH_3) and δ_H 1.34 (CH_3-26/27) to δ_C 74.6 (C-25) confirmed that the methoxy group and gem-dimethyl were linked to position C-25. The hydrolysis of **7** with 1M HCl yielded L-arabinose. The coupling constant of $J_{H\text{-}1'/H\text{-}2'}$ = 7.4 Hz of the sugar anomeric proton indicated the α-orientation for the arabinosyl group. Accordingly, the structure of **7** was established and given the common name cyclocarioside X (Figure 1).

Cyclocarioside Y (**8**) was revealed to have the molecular formula $C_{38}H_{64}O_9$ by the NMR data (^1H, ^{13}C, pyridine-d_5) and its positive-ion peak $[M + Na]^+$ at *m/z* 687.4491 (calcd. for $C_{38}H_{64}O_9Na$, 687.4448) (Figure S58) in the HRESIMS spectrum, which is 14 Da more than that of **7**. The NMR data (^1H, ^{13}C, pyridine-d_5, Tables 2 and 3) of **8** were closely analogous to those of **7**; they differed in the existence of a methyl group signals H-6'-CH_3 (δ_H 1.59, d, 6.0 Hz; δ_C 18.9) in **8**, indicating that **8** is also a 3,4-*seco*-dammarane triterpenoid saponin. In the HMBC spectrum, the correlation of H-6'-CH_3 (δ_H 1.59, d, J = 6.0 Hz) with C-5' (δ_C 73.2) indicated that H-6'-CH_3 is linked to C-5'. The HMBC correlation (Figures 2 and S40) of H-1' (δ_H 4.94) with C-12 (δ_C 76.3) indicated the linkage of the sugar unit to the 3,4-*seco*-dammarane triterpenoid

skeleton was at C-12. The hydrolysis with 1M HCl yielded quinovopyranose. The coupling constant of $J_{H\text{-}1'/H\text{-}2'}$ = 7.2 Hz suggested the quinovopyranose was *β*-oriented. Thus, the structure of **8** was elucidated and given a trivial name cyclocarioside Y (Figure 1).

Cyclocarioside Z_1 (**9**) was found to have the formula $C_{37}H_{62}O_9$ via the NMR data (^{1}H, ^{13}C, pyridine-d_5) and its negative-ion peak $[M + Cl]^-$ at *m/z* 685.4074 (calcd. for $C_{37}H_{62}ClO_9$, 685.4082) (Figure S66) in the HRESIMS, which is 14 Da less than that of **8**. The NMR data (^{1}H, ^{13}C, pyridine-d_5, Tables 2 and 3) of **9** showed that the signals were analogous to those of **8** except for the absence of an $-OCH_3$ signals (δ_H 3.23/δ_C 50.7) in **9**, suggesting that **9** is also a 3,4-*seco*-dammarane triterpenoid saponin. The NMR data (^{1}H, ^{13}C, pyridine-d_5, Tables 2 and 3, Figures 2 and S72) confirmed that an $-OCH_3$ at position C-25 in **9** was substituted with a –OH in **8**. The sugar unit was confirmed by hydrolysis to be quinovopyranose. The coupling constant of $J_{H\text{-}1'/H\text{-}2'}$ = 7.2 Hz demonstrated that the quinovopyranose was *β*-oriented. Thus, the structure of **9** was identified and given the common name cyclocarioside Z_1 (Figure 1).

Cyclocarioside Z_2 (**10**) has the same molecular formula of $C_{37}H_{62}O_9$ as **7**, as evidenced by the NMR (^{1}H, ^{13}C, pyridine-d_5) data and its negative-ion peak $[M + Cl]^-$ at *m/z* 685.4072 (calcd. for $C_{37}H_{62}ClO_9$, 685.4082) (Figure S74) in the HRESIMS spectrum. The ^{1}H- and ^{13}C-NMR data (pyridine-d_5, Tables 2 and 3) of **10** were analogous to those of **7** except for the positions of the double bond and the –OH of the side chain, indicating that **10** also possesses a 3,4-*seco*-dammarane skeleton. In its ^{1}H-^{1}H COSY spectrum (Figures 2 and S79), the correlations of H-22/H-23/H-24 suggested that there is a $-CH_2CH(O)CH{=}C$ fragment. In its HMBC spectrum (Figures 2 and S80), the correlations of H-23-OCH_3 (δ_H 3.24, s) with C-23 (δ_C 76.3) and H-24 (δ_H 5.22, d, J = 6.0 Hz) with C-25 (δ_C 135.9)/C-26 (δ_C 18.7)/C-27 (δ_C 26.2) indicated

that the methoxy group and the double bond were located at C-23 and C-24/C-25, respectively. The hydrolysis of **10** yielded L-arabinose. The α-configuration for the sugar was confirmed by its coupling constant of 7.4 Hz between H-1′ and H-2′. These findings indicated that **10** possessed a skeleton of 3,4-*seco*-dammarane triterpenoid.

Cyclocarioside Z_3 (**11**) has the molecular formula $C_{38}H_{64}O_9$ (Figure S82) by the NMR (^{1}H, ^{13}C, pyridine-d_5) data and its negative-ion peak $[M + Cl]^-$ at *m/z* 699.4222 (calcd. for $C_{38}H_{64}ClO_9$, 699.4239) in the HRESIMS spectrum, which is 14 Da more than that of **10**. The NMR (^{1}H, ^{13}C, pyridine-d_5, Tables 2 and 3) spectra of **11** suggested that its basic signals were analogous to those of **10** except for the existence of a β-D-quinovopyranosyl unit at C-12 and the absence of an α-L-arabinopyranosyl moiety at C-12. The sugar unit was determined to be a β-D-quinovopyranosyl moiety based on the hydrolysis of **11** with 1M HCl and Sigel TLC with D-quinovose and the NMR (^{1}H, ^{13}C, pyridine-d_5, Tables 2 and 3) data. The HMBC (Figures 2 and S88) correlation of H-6'-CH_3 (δ_H 1.58) with C-5' (δ_C 73.2) suggested H-6'-CH_3 linked to C-5'. The HMBC correlation of H-1' (δ_H 4.94, anomeric proton) with C-12 (δ_C 76.2) indicated that the linkage of the sugar unit to the 3,4-*seco*-dammarane skeleton was at C-12. The results revealed that **11** was also a 3,4-*seco*-dammarane triterpenoid saponin.

To determine the relative configurations of position 23 of **10** and **11**, their ROESY spectra and comparisons of the NMR (^{1}H, ^{13}C, pyridine-d_5) data with two known epimers which possess the same side chain were focused. In the ROESY spectra of **10** and **11** (Figures 3, S81 and S89), the correlations of H-23/H-21-CH_3 indicated that H-23 in each compound was α-oriented. In addition, the ^{13}C-NMR data at δ_C 127.4 (C-24), δ_C 135.9 (C-25) of **10** and at δ_C 127.5 (C-24), δ_C 136.4 (C-25) of **11** more closely resembled those at δ_C 128.4 (C-24), δ_C 135.6 (C-25) of

23β-cycloarta-24-ene-3β,23-diol than those at δ_C 129.1 (C-24), δ_C 133.8 (C-25) of 23α-cycloarta-24-ene-3β,23-diol.[27] From the above analyses, the methoxy groups in position 23 of the side chains of **10** and **11** were deduced to be β-oriented. Correspondingly, the absolute configurations of position 23 in **10** and **11** were unambiguously confirmed to be *R*. Compounds **10** and **11** were designated cyclocarioside Z_2 and cyclocarioside Z_3, respectively (Figure 1).

By comparisons of the NMR data (^{1}H, ^{13}C) to those reported in the literatures, the known isolates were identified as cyclocariol H (**12**),[10] cyclocarioside O (**13**),[28] cyclocarioside P (**14**),[28] cyclocarioside J (**15**),[29] cyclocarioside I (**16**),[16] cyclocarioside H (**17**),[11] and cyclocarioside K (**18**).[12]

The extracts and the compounds suppress the release of NO in LPS-activated RAW 264.7 cells. As shown in Figure 4, relative to the PE, EtOAc, n-Butanol, and H_2O extracts, the EtOAc fraction of the 75% EtOH-H_2O extract revealed strong inhibition to the release of NO in LPS-activated RAW 264.7 cells, comparable to the inhibition achieved by the positive control dexamethasone. Thus, the anti-inflammatory compounds were further isolated from the EtOAc fraction.

The cell viability assay showed that these compounds did not exhibit any cytotoxicity, and the survival rates of RAW 264.7 cells were over 90% at a concentration of 40 μM of each compound. Studies have shown after RAW 264.7 cells are treated with LPS, large amounts of NO, TNF-α, PGE_2 and IL-6 can be released, which result in inflammation.[30-32]

The inhibitory activities of **1-18** against LPS-activated NO release in RAW 264.7 cells are shown in Table 4. From the results, it was deduced that compounds **2**, **4**, **6-8**, **10-13**, and **16-17** suppressed the release of NO, with IC_{50} values ranging from 8.23 μM to 34.57 μM. Compounds **7**, **8**, **10**, and **11** showed strong inhibition to the

production of NO with IC_{50} values of 8.23 μM, 9.41 μM, 9.36 μM, and 11.23 μM, respectively, comparable to the inhibition achieved by the positive control dexamethasone (IC_{50}: 8.34 μM). Compounds **1**, **3**, **5**, **9**, **14-15**, and **18** showed weak inhibition of the release of NO, with IC_{50} values above 40 μM.

A comparison of the structures of these dammarane triterpenoid saponins with their activities revealed that the methoxy group in the side chain seemed to be related to high potency against LPS-activated NO release in RAW 264.7 cells. For example, among the compounds, compounds **7**, **8**, **10**, and **11**, with methoxy groups at positions 25 or 23, achieved the most effective inhibition of NO release. Moreover, the dammarane triterpenoid saponins (**1-6**, **9**, and **12-18**), without methoxy groups on the side chain, achieved reduced or no inhibition of the release of NO. Furthermore, by comparing the inhibitory activities against NO release with their structures, it was deduced that the kind of sugar group was important in influencing the inhibitory effect on NO release. Compounds **2**, **4**, **7**, and **10**, with an arabinopyranosyl moiety at position 12, exhibited stronger activity against the release of NO than their corresponding compounds **3**, **5**, **8**, and **11**, with a quinovopyranosyl moiety at position 12. Similarly, compounds **13**, with two arabinopyranosyl moieties at positions 3 and 12, revealed stronger inhibitory activities against the release of NO than their corresponding compounds **14**, with an arabinopyranosyl unit and a quinovopyranosyl unit at positions 3 and 12, respectively. Furthermore, the inhibitory activities against the release of NO were related to the absolute configurations of the side chain at positions 23 and 24. For example, compound **2** possesses different absolute configurations of the side chain at positions 23 and 24 than compounds **1** and **3** and showed higher activity than both **1** and **3**. The inhibitory activity against the release of NO was also found to be related to the substitution positions of the double bond and –

OCH_3 in the side chain. For example, the substitution positions of the double bond and $–OCH_3$ in the side chains of **7** and **8** differ from those of **10** and **11** and showed different activity. Comparison of the structures of **4** and **13** revealed that the inhibitory activity against NO release appears largely unrelated to the presence of cleavage in positions 2 and 3. In addition, comparison of the structures of **13** and **16** indicated that the inhibitory activity is related to the existence of a ring in the side chain. For example, compound **13**, without an oxygen-substituted five-member ring in the side chain, revealed weaker inhibitory effects on NO release than did compound **16**, which has a ring. In summary, the inhibitory effects of dammarane triterpenoid saponins **1-18** on the release of NO depend on the substitution of the $–OCH_3$ on the side chain, the kind of sugar, the absolute configuration of the side chain, the substitution positions of the double bond and $–OCH_3$, the cleavage in positions 2 and 3, and the presence of a ring in the side chain.

Active compounds reduce the expression of TNF-*α*, PGE_2 and IL-6 in LPS-activated RAW 264.7 cells. To explore the inhibition to inflammation of active compounds **7**, **8**, **10**, and **11**, three crucial proinflammatory mediators, TNF-*α*, PGE_2 and IL-6, were investigated whether these compounds are able to decrease these proinflammatory molecules stimulated by LPS. The levels of cytokines TNF-*α*, PGE_2, and IL-6 markedly increased after LPS treatment. However, the overexpression of cytokines TNF-*α*, PGE_2, and IL-6 was reduced by treatment with **7**, **8**, **10**, and **11** (Figures 5, 6, and 7). Generally, the results suggested that these isolates can inhibit the expression of cytokines TNF-*α*, PGE_2, and IL-6 in a concentration-dependent manner in LPS-activated RAW 264.7 cells. Notably, among the inhibitory effects of the four isolates on the expression levels of cytokines TNF-*α*, PGE_2, and IL-6, those of compound **7** were the most significant. The inhibitory activity of **7** was almost

476 equivalent to that of the positive control, dexamethasone.

477 **Compound 7 inhibits the levels of proteins COX-2, iNOS, and NF-κB/p65 in**
478 **LPS-activated RAW 264.7 cells.** NF-κB is a critical transcription factor regulating
479 proinflammatory cytokine expression during inflammation.[33-36] Moreover, proteins
480 iNOS and COX-2 are important proinflammatory mediators that contribute to
481 inflammation.[37-40] To detect the effects of active compound **7** on protein and gene
482 expression, the levels of COX-2, iNOS, and NF-κB/p65 in LPS-activated cells were
483 measured. Activated by LPS, RAW 264.7 cells exhibited markedly increased levels of
484 the proteins COX-2, iNOS, and NF-κB/p65 relative to the levels of control cells
485 (Figure 8). After treatment with compound **7**, the levels of proteins COX-2, iNOS,
486 and NF-κB/p65 in LPS-activated cells were markedly decreased. Compound **7**
487 inhibited the expression levels of proteins COX-2, iNOS, and NF-κB/p65 in
488 LPS-activated RAW 264.7 cells in a dose-dependent manner.

489 **Conclusion.** The *C. paliurus* is a famous edible medicinal plant in China, and its
490 potent anti-inflammatory effects have attracted increasing attention. However, before
491 the present study, its active anti-inflammatory compounds had not been identified. In
492 the present study, anti-inflammatory-guided isolation of the leaves of *C. paliurus*
493 identified eighteen dammarane triterpenoid glycosides, including eleven new
494 3,4-*seco*-dammarane triterpenoid glycosides (**1-11**). Bioassays demonstrated that
495 compounds **7-8** and **10-11** showed potent inhibitory effects on the expression of
496 cytokines NO, TNF-α, PGE_2, and IL-6. In addition, compound **7** significantly
497 suppressed the expression levels of proteins COX-2, iNOS, and NF-κB/p65,
498 indicating that this compound produced anti-inflammatory effects through the
499 suppression of NF-κB signaling pathways. The structure-activity relationship analysis
500 suggested that the anti-inflammatory activities of dammarane triterpenoid saponins are

correlated with the substitution of the methoxy group in the side chain, the kind of sugar, and the absolute configuration of the side chain of the compounds. In summary, *C. paliurus* contains abundant anti-inflammatory dammarane triterpenoid saponins, and compound **7** is a promising natural anti-inflammatory drug that warrants further investigation. These findings suggest that regular consumption of the leaves of *C. paliurus* may help prevent the occurrence of inflammatory diseases.

ASSOCIATED CONTENT

Supporting Information

The Supporting Information is available free of charge on the ACS Publications website at DOI: xxxxxx. ^{1}H NMR, ^{13}C NMR, DEPT, HSQC, ^{1}H-^{1}H COSY, HMBC, ROESY and HRESIMS spectra for compounds **1**−**11** (PDF).

AUTHOR INFORMATION

Corresponding Authors

*E-mail: lijun9593@gxnu.edu.cn.

*E-mail: huangxishan13@foxmail.com.

ORCID

Jun Li: 0000-0003-2023-8609

Notes

The authors declare no competing financial interest.

ACKNOWLEDGMENTS

This research was supported by National Natural Science Foundation of Guangxi (21662004), the Province Natural Science Foundation of Guangxi (2018JJD140035

526 and 2018JJA140613) and the Key Laboratory for the Chemistry and Molecular
527 Engineering of Medicinal Resources (CMEMR2019-A1).

528

529 **REFERENCES**

530 (1) Jin, L.; Li, X. B.; Tian, D. Q.; Fang, X. P.; Yu, Yong-Ming M.; Zhu, H. Q.; Ge, Y. Y.; Ma,
531 G. Y.; Wang, W. Y.; Xiao, W. F. Antioxidant properties and color parameters of herbal teas in
532 China. *Ind. Crop. Prod.* **2016**, *87*, 198-209.

533 (2) Ning, Z. W.; Zhai, L. X.; Huang, T.; Peng, J.; Hu, D.; Xiao, H. T.; Wen, B.; Lin, C. Y.;
534 Zhao, L.; Bian, Z. X. Identification of α-glucosidase inhibitors from *cyclocarya paliurus* tea leaves
535 using UF-UPLC-Q/TOF-MS/MS and molecular docking. *Food Funct.* **2019**, *10*, 1893-1902.

536 (3) Xiao, H. T.; Wen, B.; Ning, Z. W.; Zhai, L. X.; Liao, C. H.; Lin, C. Y.; Mu, H. X.; Bian, Z.
537 X. *Cyclocarya paliurus* tea leaves enhances pancreatic β cell preservation through inhibition of
538 apoptosis. *Sci. Rep.* **2017**, *7*, 1-13.

539 (4) Xie, J. H.; Xie, M. Y.; Nie, S. P.; Shen, M. Y.; Wang, Y. X.; Li, C. Isolation, chemical
540 composition and antioxidant activities of a water-soluble polysaccharide from *Cyclocarya*
541 *paliurus* (Batal.) Iljinskaja. *Food Chem.* **2010**, *119*, 1626-1632.

542 (5) Wang, Q. Q.; Jiang, C. H.; Fang, S. Z.; Wang, J. H.; Ji, Y.; Shang, X. L.; Ni, Y. C.; Yin, Z.
543 Q.; Zhang, J. Antihyperglycemic, antihyperlipidemic and antioxidant effects of ethanol and
544 aqueous extracts of *Cyclocarya paliurus* leaves in type 2 diabetic rats. *J. Ethnopharmacol.* **2013**,
545 *150*, 1119-1127.

546 (6) Zhang, J.; Shen, Q.; Lu, J. C.; Li, J. Y.; Liu, W. Y.; Yang, J. J.; Li, J.; Xiao, K. Phenolic
547 compounds from the leaves of *Cyclocarya paliurus* (Batal.) Ijinskaja and their inhibitory activity
548 against PTP1B. *Food Chem.* **2010**, *119*, 1491-1496.

549 (7) The National Health Commission of the people's Republic of China. Eight new raw
550 materials for foods, such as *Euglena gracilis*. *Bulletin of The National Health Commission of the*
551 *people's Republic of China*. **2013**, *124,* 4.

552 (8) Yang, H. M.; Yin, Z. Q.; Zhao, M. G.; Jiang, C. H.; Zhang, J.; Pan, K. Pentacyclic
553 triterpenoids from *Cyclocarya paliurus* and their antioxidant activities in FFA-induced HepG2

554 steatosis cells. *Phytochemistry* **2018**, *151*, 119-127.

555 (9) Fang, Z. J.; Shen, S. N.; Wang, J. M.; Wu, Y. J.; Zhou, C. X.; Mo, J. X.; Lin, L. G.; Gan, L.
556 S. Triterpenoids from *Cyclocarya paliurus* that enhance glucose uptake in 3T3-L1 adipocytes.
557 *Molecules* **2019**, *24*, 187.

558 (10) Chen, Y. J.; Na, L.; Fan, J. L.; Zhao, J. P.; Hussain, N.; Jian, Y. Q.; Yuan, H. W.; Li, B.;
559 Liu, B.; Choudhary, M. I.; Khan, I.; Wang, W. Seco-dammarane triterpenoids from the leaves of
560 *Cyclocarya paliurus. Phytochemistry* **2018**, *145*, 85-92.

561 (11) Li, S.; Cui, B. S.; Liu, Q.; Tang, L.; Yang, Y. C.; Jin, X. J.; Shen, Z. F. New triterpenoids
562 from the leaves of *Cyclocarya paliurus*. *Planta Med.* **2012**, 78, 290-296.

563 (12) Cui, B. S.; Li, S. New triterpenoids saponins from the leaves of *Cyclocarya paliurus*. *Chin.*
564 *Chem. Lett.* **2015**, *26*, 585-589.

565 (13) Xuan, T. Y.; Tan, J.; Sun, H. H.; Yang, C.; Lv, W. Y.; Zhang, J. H.; Zhang, K. Q.; Nie, Z.
566 Q.; Ye, Z. J.; He, X. A.; Zhu, G. Z.; Xu, K. P. Cyclocarioside O-Q, three novel seco-dammarane
567 triterpenoid glycosides from the leaves of *Cyclocarya paliurus*. *Nat. Prod. Res.* **2019**.
568 Doi.org/10.1080/14786419.2019.1616722.

569 (14) Wu, Y.; Li, Y. Y.; Wu, X.; Gao, Z. Z.; Liu, C.; Zhu, M.; Song, Y.; Wang, D. Y.; Liu, J. G.;
570 Hu, Y. L. Chemical constituents from *Cyclocarya paliurus* (Batal.) Iljinsk. *Biochem. Systemat.*
571 *Ecol.* **2014**, *57*, 216-220.

572 (15) Shu, R. G.; Xu, C. R.; Li, L. N.; Yu, Z. L. Cyclocariosides II and III: two seco-dammarane
573 triterpenoid saponins from *Cyclocarya paliurus*. *Planta Med*. **1995**, *61*, 551-553.

574 (16) Kennelly, E. J.; Cai, L.; Long, L.; Shamon, L.; Zaw, K.; Zhou, B. N.; Pezzuto, J. M.;
575 Kinghorn, A. D. Novel highly sweet seco-dammarane glycosides from *Pterocarya paliurus*. *J.*
576 *Agric. Food Chem.* **1995**, *43*, 2602-2607.

577 (17) Zhu, K. N.; Jiang, C. H.; Tian, Y. S.; Xiao, N.; Wu, Z. F.; Ma, Y. L.; Lin, Z.; Fang, S. Z.;
578 Shang, X. L.; Liu, K. Two triterpenoids from *Cyclocarya paliurus* (Batal) Iljinsk (Juglandaceae)
579 promote glucose uptake in 3T3-L1 adipocytes: the relationship to AMPK activation.
580 *Phytomedicine* **2015**, *22*, 837-846.

581 (18) Jiang, C. H.; Yao, N.; Wang, Q. Q.; Zhang, J. H.; Sun, Y.; Xiao, N.; Liu, K.; Huang, F.;
582 Fang, S. Z.; Shang, X. L.; Liu, B. L.; Ni, Y. C.; Yin, Z. Q.; Zhang, J. *Cyclocarya paliurus* extract

583 modulates adipokine expression and improves insulin sensitivity by inhibition of inflammation in
584 mice. *J. Ethnopharmacol*. **2014**, *153*, 344-351.
585 (19) Liu, S. H.; Lin, C. H.; Hung, S. K.; Chou, J. H.; Chi, C. W.; Fu, S. L. Fisetin inhibits
586 lipopolysaccharide-induced macrophage activation and dendritic cell maturation. *J. Agric. Food*
587 *Chem.* **2010**, *58*, 10831-10839.
588 (20) Shen, C. Y.; Zhang, T. T.; Zhang, W. L.; Jiang, J. G. Anti-inflammatory activities of
589 essential oil isolated from the calyx of *Hibiscus sabdariffa L. Food Funct.* **2016**, *7*, 4451-4459.
590 (21) Shen, C. Y.; Jiang, J. G.; Li, M. Q.; Zheng, C. Y.; Zhu, W. Structural characterization and
591 immunomodulatory activity of novel polysaccharides from *Citrus aurantium Linn.* variant amara
592 Engl. *J. Funct. Foods* **2017**, *35*, 352-362.
593 (22) McChesney, J. D.; Dou, J.; Sindelar, R. D.; Goins, D. K.; Walker, L. A.; Rogers, R. D.
594 Tirucallane-type triterpenoids: nmr and X-ray diffraction analyses of 24-*epi*-piscidinol A and
595 piscidinol A. *J. Chem. Cryst*. **1997**, *27*, 283-290.
596 (23) Kazufumi, T.; Takafumi, N.; Takashi, O.; Midori, A. A.; Takashi, K.; Thaworn, K.;
597 Masami I. *Cycloartane triterpenes* isolated from *Combretum quadrangulare* in a screening
598 program for death-receptor expression enhancing activity. *J. Nat. Prod.* **2011**, *74*, 249-255.
599 (24) Joycharat, N.; Greger, H.; Hofer, O.; Saifah, E. Flavaglines and triterpenoids from the
600 leaves of *Aglaia forbesii. Phytochemistry* **2008**, *69*, 206-211.
601 (25) Dirsch, V. M.; Stuppner, H.; Vollmar, A. M. The Griess assay: suitable for a bio-guided
602 fractionation of anti-inflammatory plant extracts. *Planta Med.* **1998**, *64*, 423-426.
603 (26) Yoshikawa, M.; Hatakeyama, S.; Tanaka, N.; Fukuda, Y.; Yamahara, J.; Murakami, N.
604 Crude drugs from aquatic plants. I. On the constituents of *Alismatis Rhizoma.* (1). Absolute stereo
605 structures of alisols E 23-acetate, F, and G, three new protostane-type triterpenes from Chinese
606 *Alismatis Rhizoma*. *Chem. Pharm. Bull.* **1993**, *41*, 1948-1954.
607 (27) Lago, J. H. G.; Brochini, C. B.; Roque, N. F. Terpenoids from *Guarea guidonia*.
608 *Phytochemistry* **2002**, *60*, 333-338.
609 (28) Wang, Y. R.; Cui, B. S.; Han, S. W.; Li, S. New dammarane triterpenoid saponins from the
610 leaves of *Cyclocarya paliurus. J. Asian. Nat. Prod. Res.* **2018**, *20*, 1019-1027.
611 (29) Liu, Y.; Zhang, M. Q.; Li, X. L.; Xu, T. H.; Xie, S. X.; Xu, Y. J.; Xu, D. M. Study on

612 chemical constituents of *Cyclocarya paliurus*. *J. Asian. Nat. Prod. Res.* **2014**, *16*, 206-209.

613 (30) Coulter, J. A.; McCarthy, H. O.; Xiang, J.; Roedi, W.; Wagner, E.; Robson, T.; Hirst, D. G.
614 Nitric oxide-A novel therapeutic for cancer. *Nitric Oxide* **2008**, *19*, 192-198.

615 (31) Wu, Y. L.; Han F.; Luan S. S.; Ai R.; Zhang P.; Li H.; Chen L. X. Triterpenoids from
616 *Ganoderma lucidum* and their potential anti-inflammatory effects. *J. Agric. Food Chem.* **2019**, *67*,
617 5147-5158.

618 (32) Liu, Z. G.; Tang, L. G.; Zhu, H. P.; Xu, T. T.; Qiu, C. Y.; Zheng, S. Q.; Gu, Y. G.; Feng, J.
619 P.; Zhang, Y. L.; Liang, G. Design, synthesis, and structure–activity relationship study of novel
620 indole-2-carboxamide derivatives as anti-inflammatory agents for the treatment of Sepsis. *J. Med.*
621 *Chem.* **2016**, *59*, 4637-4650.

622 (33) Liu, Z. K.; Ng, C. F.; Shiu, H. T.; Wong, H. L.; Wong, C. W.; Li, K. K. A traditional
623 Chinese formula composed of Chuanxiong rhizoma and *Gastrodiae Rhizoma* (Da Chuanxiong
624 Formula) suppresses inflammatory response in LPS -induced RAW 264.7 cells through inhibition
625 of NF-κB pathway. *J. Ethnopharmacol.* **2017**, *196*, 20-28.

626 (34) Tak, P. P.; Firestein, G. S. NF-κB a key role in inflammatory diseases. *J. Clin. Invest.*
627 **2001**, *107*, 7-11.

628 (35) Zhai, X. T.; Zhang, Z. Y.; Jiang, C. H.; Chen, J. Q.; Ye, J. Q.; Jia, X. B.; Yang, Y.; Ni, Q.;
629 Wang, S. X.; Song, J.; Zhu, F. X. Nauclea officinalis inhibits inflammation in LPS-mediated
630 RAW 264.7 macrophages by suppressing the NF-κB signaling pathway. *J. Ethnopharmacol.* **2016**,
631 *183*, 159-160.

632 (36) Liu, Z. W.; Fan, Y. M.; Wang, Y.; Han, C.; Pan, Y.; Huang, H.; Ye, Y.; Luo, L.; Yin, Z.
633 M. Dipyrithione inhibits lipopolysaccharide-induced iNOS and COX-2 up-regulation in
634 macrophages and protects against endotoxic shock in mice. *Febs. Lett.* **2008**, *582*, 1643-1650.

635 (37) Moona, D. O.; Kima, M. O.; Lee, J. D.; Choi, Y. H.; Kim, G. Y. Rosmarinic acid sensitizes
636 cell death through suppression of TNF-α-induced NF-*κ*B activation and ROS generation in human
637 leukemia U937 cells. *Cancer Lett.* **2010**, *288*, 183-191.

638 (38) Killeen, M. J.; Linder, M.; Pontoniere, P.; Crea, R. NF-*κ*B signaling and chronic
639 inflammatory diseases: exploring the potential of natural products to drive new therapeutic
640 opportunities. *Drug Discov. Today* **2014**, *19*, 373-378.

641 (39) Hayden, M. S.; Ghosh, S. Shared principles in NF-kappaB signaling. *Cell* **2008**, *132*,
642 344-362.
643 (40) Gupta, S. C.; Sundaram, C.; Reuter, S.; Aggarwa, B. B. Inhibiting NF-κB activation by
644 small molecules as a therapeutic strategy. *Biochim. Biophys. Acta, Gene Regul. Mech*. **2010**, *1799*,
645 775-787.

Captions of Figures

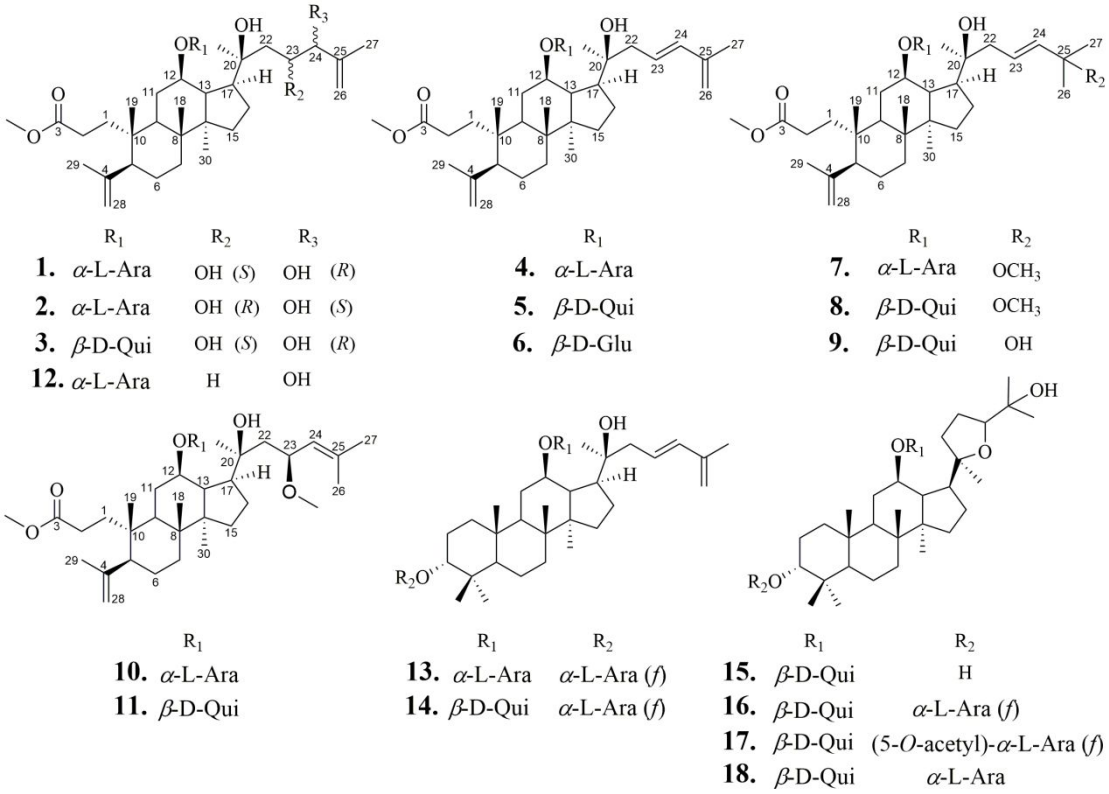

Figure 1. Structures of compounds **1**−**18** isolated from the leaves of *C. paliurus*

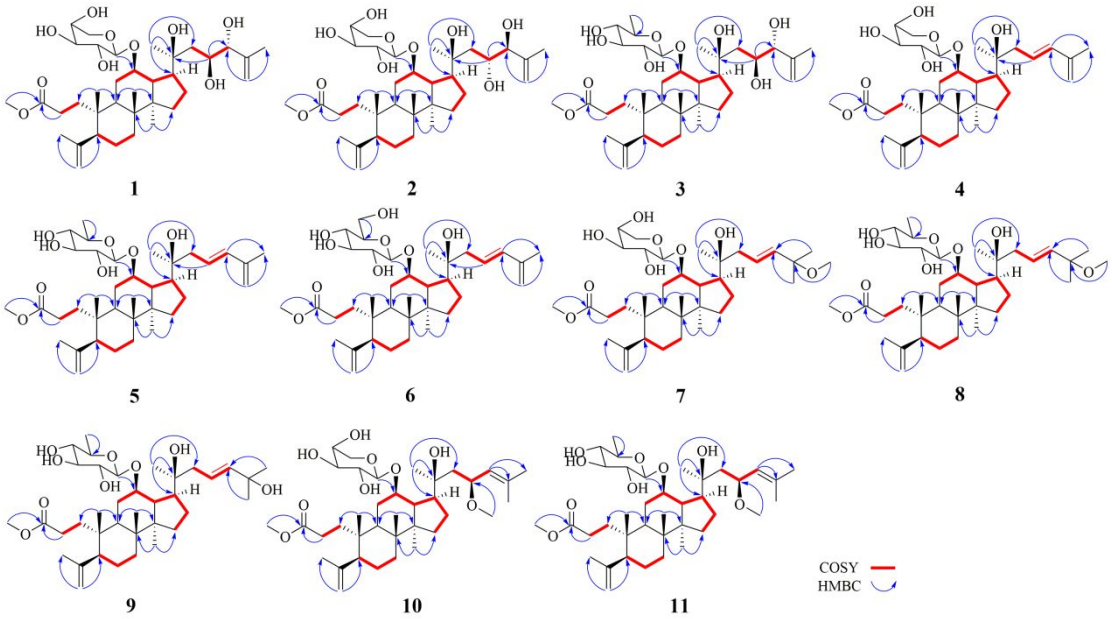

Figure 2. Key HMBC and COSY correlations of compounds **1**−**11**

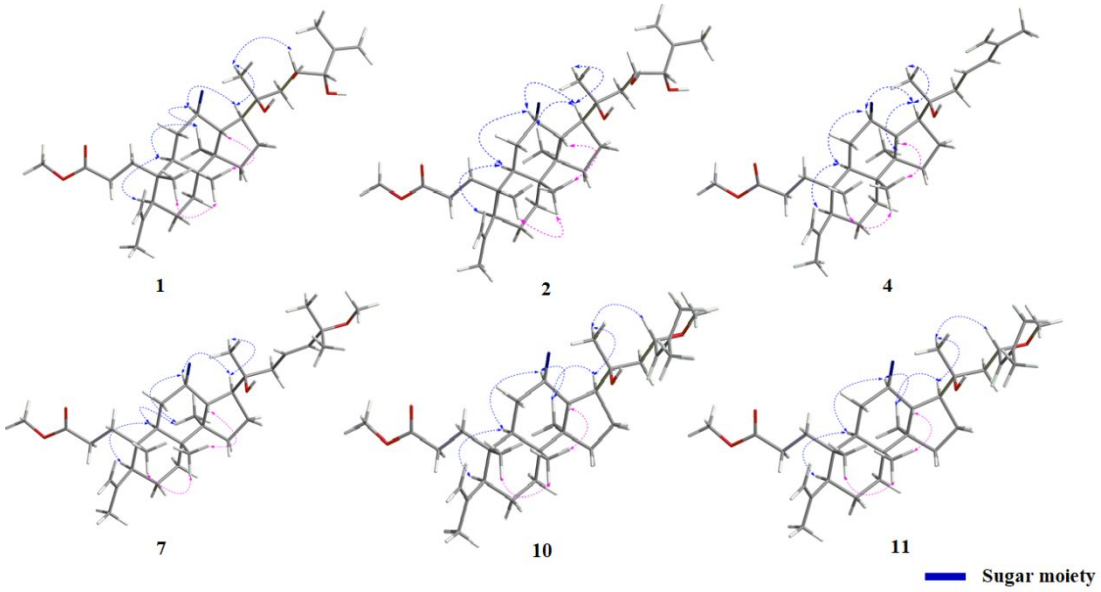

Figure 3. ROESY correlations of compounds **1**, **2**, **4**, **7**, **10**, and **11**

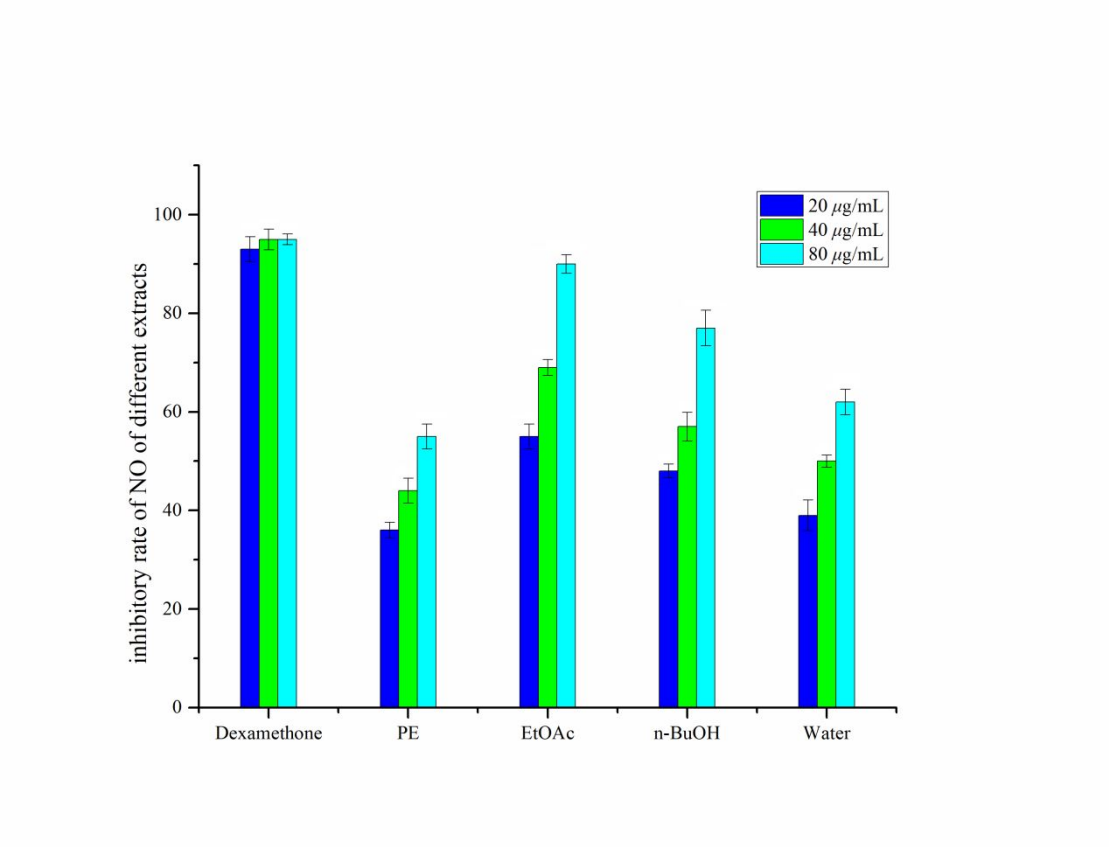

Figure 4. Inhibitory effects against NO of the different fractions in LPS-activated RAW 264.7 cells

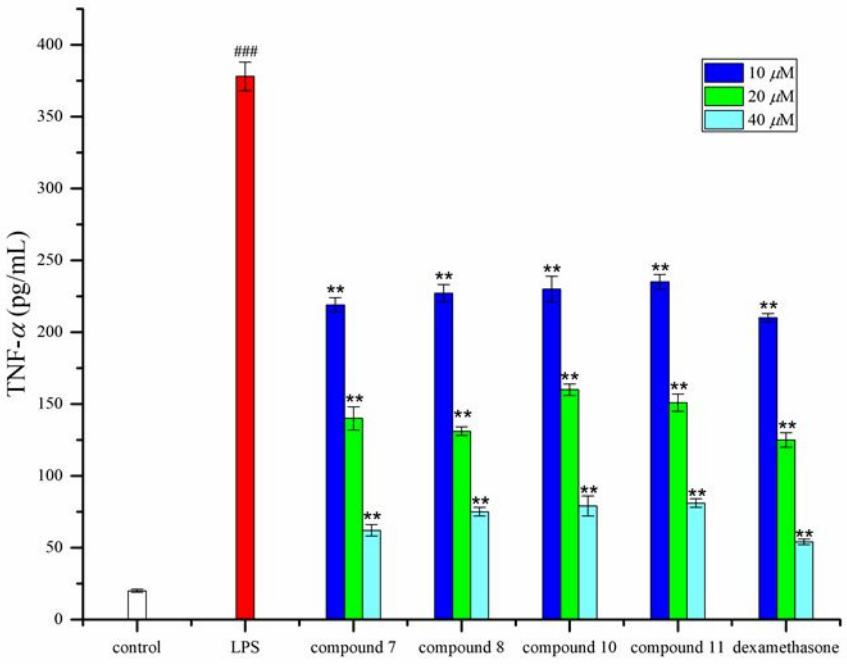

Figure 5. Inhibitory activities of compounds **7**-**8** and **10**-**11** on TNF-α expression in LPS-activated RAW 264.7 cells. The cells were activated with LPS (100 ng/mL) for 2 h and then treated with the compounds **7**-**8** and **10**-**11** (10, 20, and 40 μM) for 24 h. The TNF-α concentration in the supernatants was measured by ELISA kits. Dexamethasone was used as a positive control at the same concentration as the compounds. Values are the mean ± SD of three independent tests. $^{###}$ $p < 0.001$ compared with the control that was induced without LPS. ** $p < 0.01$ compared with cells treated with LPS.

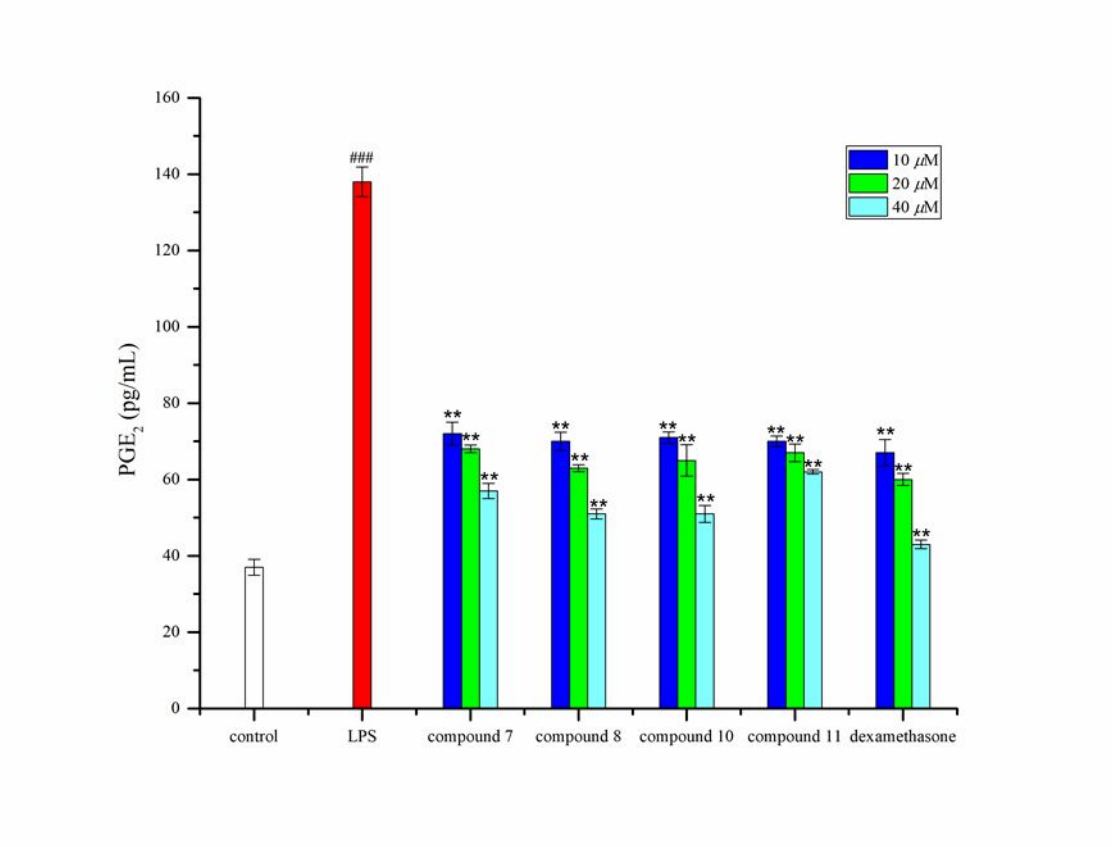

Figure 6. Effects of compounds **7-8** and **10-11** on PGE_2 expression by LPS-activated RAW 264.7 cells. The cells were activated with LPS (100 ng/mL) for 2 h and then treated with the compounds **7-8** and **10-11** (10, 20, and 40 μM) for 24 h. The PGE_2 concentration in the supernatants was determined by ELISA kits. Dexamethasone was used as a positive control at the same concentration as the compounds. Values are the mean ± SD of three independent tests. ### $p < 0.001$ compared with the control that was induced without LPS. ** $p < 0.01$ compared with cells treated with LPS.

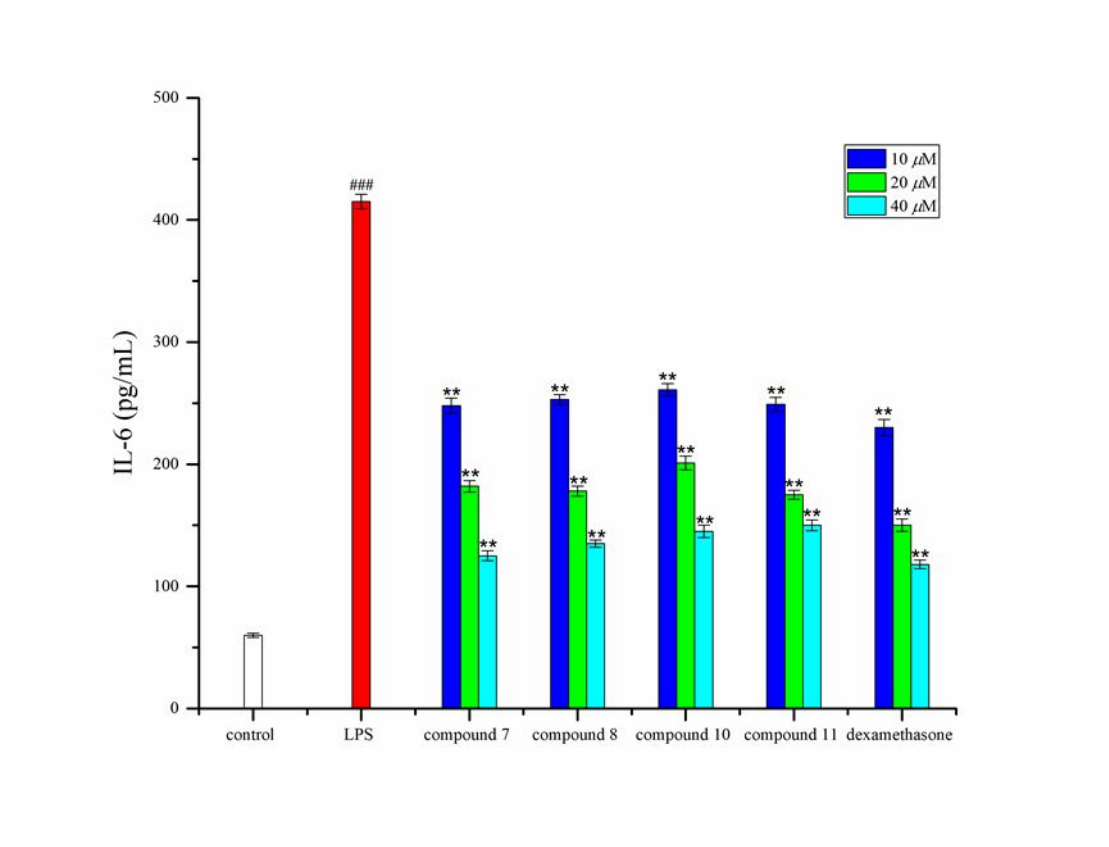

Figure 7. Effects of compounds **7-8** and **10-11** on IL-6 expression by LPS-activated RAW 264.7 cells. The cells were activated with LPS (100 ng/mL) for 2 h and then treated with the compounds **7-8** and **10-11** (10, 20, and 40 μM) for 24 h. The IL-6 concentration in the supernatants was tested by ELISA kits. Dexamethasone was used as a positive control at the same concentration as the compounds. Values are the mean ± SD of three independent tests. $^{###}$ $p < 0.001$ compared with the control that was induced without LPS. ** $p < 0.01$ compared with cells treated with LPS.

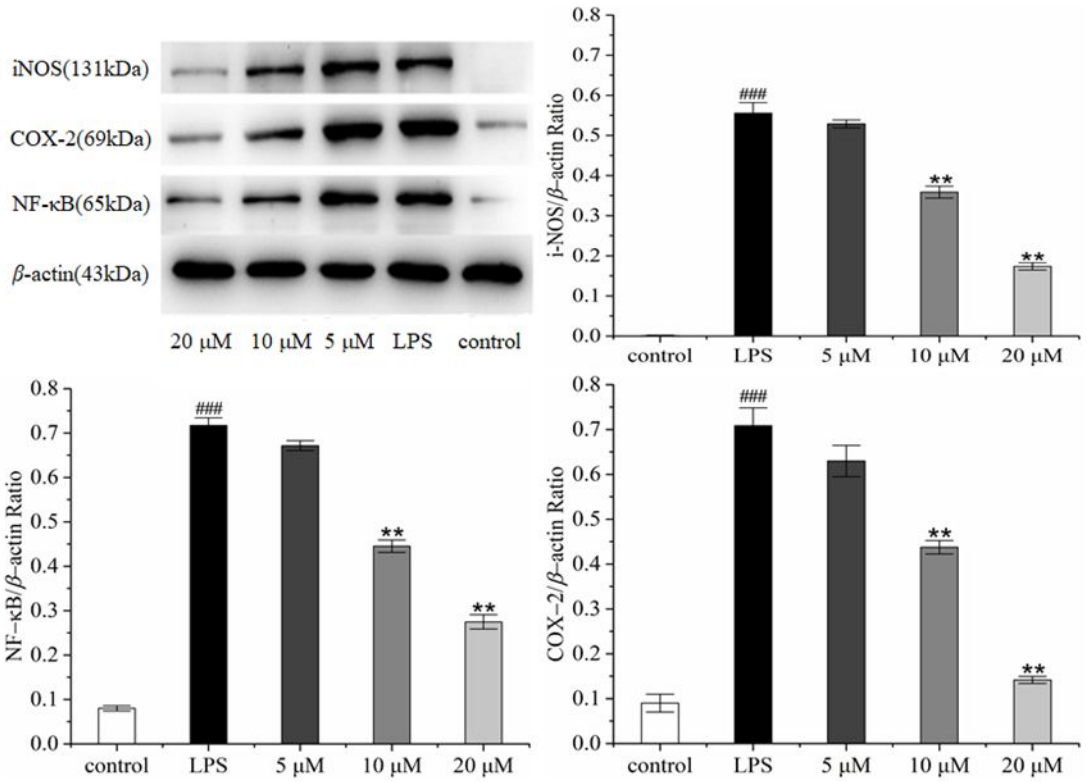

Figure 8. Effects of compound **7** at concentrations of 5, 10, and 20 μM on iNOS, COX-2, and NF-κB/p65 expression in LPS-activated RAW 264.7 cells. β-Actin served as the loading control. ### $p < 0.001$ compared with the control that was activated without LPS. ** $p < 0.01$ compared with cells treated with LPS.

Captions of Tables

Table 1. ^{1}H NMR Data for Compounds **1**–**6** (500 MHz, Pyridine-d_5, δ in ppm)

Table 2. ^{1}H NMR Data for Compounds **7**–**11** (500 MHz, Pyridine-d_5, δ in ppm)

Table 3. ^{13}C NMR Data for Compounds **1**–**11** (125 MHz, Pyridine-d_5, δ in ppm)

Table 4. Inhibitory Activities on NO of Compounds in LPS-activated RAW 264.7 Cells

Table of Contents Graphic

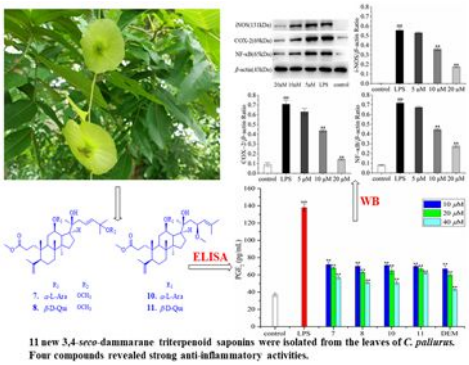

11 new 3,4-*seco*-dammarane triterpenoid saponins were isolated from the leaves of *C. pallurus*. Four compounds revealed strong anti-inflammatory activities.